


Influence of Hydrogen Pressure on the Structure of Platinum-Titania Catalysts

Journal Article

Author(s):

Beck, Arik; Frey, Hannes; Becker, Matthias; Artiglia, Luca; Willinger, Marc ; van Bokhoven, Jeroen A.

Publication date:

2021-10-21

Permanent link:

<https://doi.org/10.3929/ethz-b-000515061>

Rights / license:

[Creative Commons Attribution-NonCommercial-NoDerivatives 4.0 International](#)

Originally published in:

The Journal of Physical Chemistry C 125(41), <https://doi.org/10.1021/acs.jpcc.1c05939>

Funding acknowledgement:

178943 - Catalyst structures in three dimensions (SNF)

Influence of Hydrogen Pressure on the Structure of Platinum–Titania Catalysts

Published as part of *The Journal of Physical Chemistry virtual special issue “125 Years of The Journal of Physical Chemistry”*.

Arik Beck, Hannes Frey, Matthias Becker, Luca Artiglia, Marc G. Willinger, and Jeroen A. van Bokhoven*

Cite This: *J. Phys. Chem. C* 2021, 125, 22531–22538

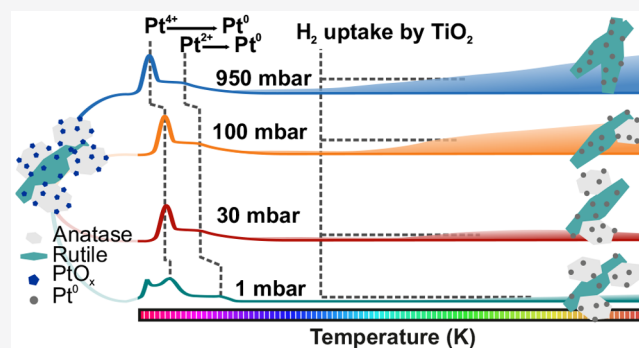
Read Online

ACCESS |

Metrics & More

Article Recommendations

ABSTRACT: Dependent on the application or characterization method catalysts are exposed to different gas pressures, which results in different structures. The quantitative determination of the structure and composition of a catalyst as a function of its gas environment allows the establishment of structure–performance relationships. Herein, we determine the structure of a platinum–titania catalyst under hydrogen during temperature-programmed reduction over 3 orders of magnitude in pressure, from 1 to 950 mbar. The pressure significantly influences the hydrogen uptake kinetics and the consecutive structural transformations of the platinum–titania catalyst. The reduction of the platinum precursor becomes pressure-independent above 30 mbar. Yet, the related spillover and stability of adsorbed hydrogen on the titania are a function of pressure. Higher pressures promote higher hydrogen uptake and prevent desorption of hydrogen from the catalyst. The hydrogen uptake triggers a phase transformation of anatase to rutile which is, as a result, pressure dependent. The presented systematic approach establishes a pressure–structure relation which can be applied for the catalyst treatment and to frame existing results on the catalytic system. Treating the same material at two different pressures will lead to different structures.

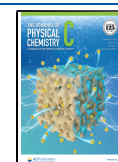


INTRODUCTION

The performance of a material depends on the structure it has under the conditions of operation. For example, heterogeneous catalysts are developed for a specific chemical transformation. To relate their structure to their performance, an understanding of the structure under the process conditions is required. Based on this structure–performance relation,^{1–3} the catalyst and process can be improved by a rational modification of the catalyst formulation, the pretreatment, and the process conditions. In the past decades, in situ and operando characterization methods emerged, which provide detailed structural information about a catalyst while being exposed to relevant conditions.⁴ Some of those techniques—especially those which rely on electron detection or use electrons as a probe—suffer limitation with respect to the maximum applicable pressure. The routinely applicable pressure of ambient pressure X-ray photoemission spectroscopy (XPS) is in the 1–50 mbar range,⁵ and in situ transmission electron microscopy operates commonly at a pressure of 1 bar.⁶ Often, however, much lower pressures are employed.^{7,8} Because some of the most important industrial applications of catalysts require pressures of well above 10 bar,^{9–11} a gap between in situ characterization and real-life process conditions

exists.¹² This pressure gap problem is well-known.¹³ The prediction of the structure as a function of pressure is nontrivial. Thermodynamics dictates what the possible structures are; however, the thermodynamically most stable structure may not evolve within a reasonable time scale because transformation kinetics can be strongly pressure related. Consequently, the pressure gap represents also a materials gap. Yet, systematic studies on the effect of pressure on real catalysts are rare.¹⁴ Recently, we performed such a systematic study for the copper–zinc–alumina catalyst and showed how seemingly contradicting theories on the catalyst’s active state can be traced back to the pressure gap to a large extent.¹⁵ Such investigations have to be expanded to other catalytic systems.

Received: July 3, 2021
Revised: August 24, 2021
Published: October 11, 2021



Platinum nanoparticles supported on metal oxides catalyze essential catalytic hydrogenation and oxidation reactions.^{16,17} Reduction in a hydrogen atmosphere is in many such applications a pretreatment to transform platinum into the active metallic state. Especially when platinum is supported on reducible metal oxides like titania (titanium(IV) dioxide), the interaction between metal and support can result in a variety of structural transformations. Potentially most prominent is the encapsulation of platinum by a thin titania overlayer when a platinum–titania catalyst is exposed to hydrogen at elevated temperature,^{18,19} the so-called strong metal–support interaction (SMSI). Varying the reduction temperature alters the structure of the catalyst to an extent that, for example, the catalytic selectivity is affected.^{20,21} It is illusive to assume that such transformations are independent from the applied partial pressure of hydrogen given the kinetic and thermodynamic dependence of any material transformation.

To understand to which degree the interaction of hydrogen with a platinum–titania catalyst depends on the pressure, here, we cross the hydrogen pressure range by 3 orders of magnitude from 1 to 950 mbar by using temperature-programmed experiments. Two platinum loadings (0.5 and 1.0 wt % Pt/TiO₂) were compared to evaluate the influence of the surface density of platinum. At low temperatures (<523 K), the behavior is independent of the hydrogen pressure; however, beyond 573 K a different interaction behavior is found which leads to differences in the resulting structure of both platinum and titania.

METHODS AND MATERIALS

Sample Preparation. Titanium(IV) dioxide Aerioxide P25 (Acros Organics (ACR)) was used as support material. The titanium dioxide was calcined in static air in a muffle furnace at 873 K for 12 h. After calcination, the support BET surface area, determined via nitrogen physisorption, was 48 m² g⁻¹. Two platinum-loaded materials were synthesized with a platinum loading of 0.5 and 1.0 wt %. Electrostatic adsorption was used to deposit the platinum precursor (tetraammineplatinum(II) nitrate, 99.995%, Sigma-Aldrich) on the titanium dioxide surface. The respective amount of precursor was dissolved in ultrapure water, the amount of which was adjusted to the support surface area (5000 m² L⁻¹). Then the pH value of the solution was adjusted by using ammonia to an initial pH value of 14. The titanium dioxide was added to the aqueous solution; the flask was covered and stirred for 24 h. Then the cover was removed to slowly evaporate water for 48 h. Finally, the materials were calcined at 623 K in static air for 1 h (heating ramp 5 K min⁻¹).

Temperature-Programmed Reduction (TPR). The application of a temperature–conductivity detector (TCD) in combination with precondensation of water allows quantification of the hydrogen uptake. Reduction experiments in a hydrogen atmosphere were performed with a Micromeritics AutoChem HP analyzer equipped with a temperature–conductivity detector (TCD). For each experiment, a total flow of gas was kept at 10 mL min⁻¹. During the analysis, the gas flowed through a cold trap cooled with an ice–liquid slurry of isopropanol (184 K) to condense water produced by the reduction before the gas reaches the TCD detector. For each experiment 100–160 mg of the material was loaded into a U-shaped stainless-steel reactor tube. The sample was fixed between two quartz wool plugs. Prior to each TPR experiment, the sample was pretreated under a flow of He (50 mL min⁻¹)

for 30 min at 373 K (ramp 20 K min⁻¹) to desorb loosely bound water from the sample surface. Subsequently, the sample was cooled to 223 K and equilibrated for 30 min. Then, the gas atmosphere was changed to 950 mbar of hydrogen, and the sample was exposed to that mixture for 30 min at 223 K. This low-temperature pretreatment was applied to perform the TPR experiments from a common starting point. After this treatment the gas atmosphere was switched to a gas mixture of the desired partial hydrogen pressure. Consequently, the sample environment was allowed to equilibrate for 20 min. Then the TPR experiment was started, and the sample tube was heated to 973 K with a heating ramp of 10 K min⁻¹. The different gas compositions were produced by using three different hydrogen mixtures, i.e., 0.01% H₂/He, 10% H₂/Ar, and 95% H₂/Ar. These gas mixtures were used for a partial hydrogen pressure of 1, 100, and 950 mbar. The partial pressure of 30 mbar was produced by mixing the 10% H₂/Ar gas with Ar with a ratio of 3:7. The total flow was kept constant at 10 mL min⁻¹ for each experiment. The experiments were at minimum performed twice to ensure reproducibility.

Transmission Electron Microscopy (TEM). TEM micrographs were acquired by using a JEOL Grand ARM 300 aberration-corrected microscope operating at 300 kV. The average size distribution was analyzed with the ferret diameter of elliptical shapes ($N = 200$).

In Situ X-ray Photoemission Spectroscopy (XPS). In situ XPS measurements were performed at the X07DB In Situ Spectroscopy beamline (Swiss Light Source, Villigen, Switzerland). The powder samples were dispersed in ultrapure water and drop-casted on a silver foil (Aldrich, 99.99% purity). The samples were introduced into the solid–gas interface end station, which allows dosing of gas under flow conditions.^{5,22} Ultrapure gases were dosed by means of mass flow controllers and pumped away with a tunable diaphragm valve connected to a root pump. This allows the dosing of gas flows and a control of the pressure during the experiments. The pressure was monitored by means of Baratron measurement heads. The purity of the gases and the switches from oxygen to nitrogen to hydrogen were controlled by a quadrupole mass spectrometer (QMS), located in the second differential pumping stage of the analyzer. The samples were heated by using a tunable infrared laser (976 nm, maximum power 25 W), which hit the back of the sample, and the temperature was monitored with a Pt100 sensor. Photoemission spectra were acquired with linearly polarized light by using an excitation energy of 1000 eV at a pass energy of 20 eV. The resulting spectra were fitted by using a Shirley background and by using a Gaussian–Lorentzian peak shape with an applied asymmetry for the metallic platinum Pt 4f peak. The asymmetry parameters were determined fitting a pure platinum foil measured in the same instrument under vacuum conditions.

X-ray Diffraction (XRD). Powder XRD was performed on a lab-b d XRD X'P Pro device from Malvern Analytical equipped with a copper X-ray source (Cu K $\alpha = 1.54$ Å).

RESULTS

Figure 1 shows the temperature-programmed reduction (TPR) profiles of the two Pt/TiO₂ catalysts and a titania P25 reference sample at four different hydrogen pressures. Hydrogen uptake can occur either via adsorption and/or incorporation of hydrogen into the catalyst structure or by the formation of water following the removal of oxygen from the catalyst. However, the TCD signal is always a superposition of

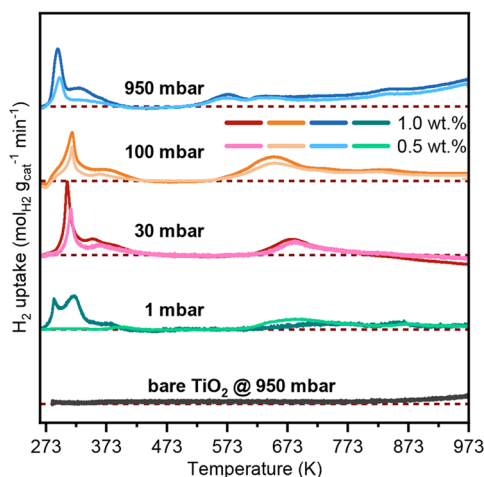


Figure 1. Temperature-programmed reduction. Hydrogen uptake profiles of 0.5 and 1.0 wt % Pt/TiO₂ during heating at different hydrogen partial pressures. As a reference TiO₂ P25 sample at 950 mbar.

hydrogen desorption and hydrogen uptake.²³ Therefore, negative hydrogen uptake can be detected and corresponds to the release of hydrogen from the catalyst. An examination of the TPR profile of pure titania (P25) under 950 mbar of hydrogen shows no significant hydrogen uptake below 773 K (Figure 1). Beyond this temperature, there is a low uptake, which increases with temperature. The platinum–titania catalysts show a very different behavior. Already at low

temperatures there is much higher hydrogen uptake observed which continues over the full temperature range with distinctive uptake features. Below 473 K, the TPR shows similar peak shapes at pressures of 30 mbar and above. The exceptional case of 1 mbar will be discussed at a later point. Between 273 and 373 K, the first major hydrogen uptake occurs for both platinum loadings. This uptake is composed of two peaks: one sharp peak at 290–315 K and a second broader one with the center at 330–380 K. The total uptake of this first region is around 0.052 and 0.031 mmol_{H₂} g⁻¹ for the 1.0 and 0.5 wt % Pt catalyst, respectively. This corresponds to a hydrogen to platinum ratio of 1.1 and 1.2 for 1.0 and 0.5 wt %. The hydrogen uptake is potentially not exclusively due to platinum oxide reduction; hydrogen spillover to the support or interfacial reduction of the titania can also contribute to this hydrogen uptake.^{24,25}

In between 393 and 493 K, the hydrogen uptake drops to zero at all pressures. Beyond this temperature, hydrogen uptake is increasing again. At 950 mbar of hydrogen, this occurs at the lowest temperature and at increasingly higher temperatures with lower pressure. The uptake can be characterized by a broad peak spanning about 100 K. Following this peak, the reduction pattern depends on the applied hydrogen pressure. At 30 mbar, the initial uptake peak is followed by a negative uptake signal which indicates that hydrogen is released from the sample by desorption. At 100 mbar, the uptake signal is slowly decreasing over the experiment, however always being positive. Only at 950 mbar is the uptake continuously increasing up to the maximum

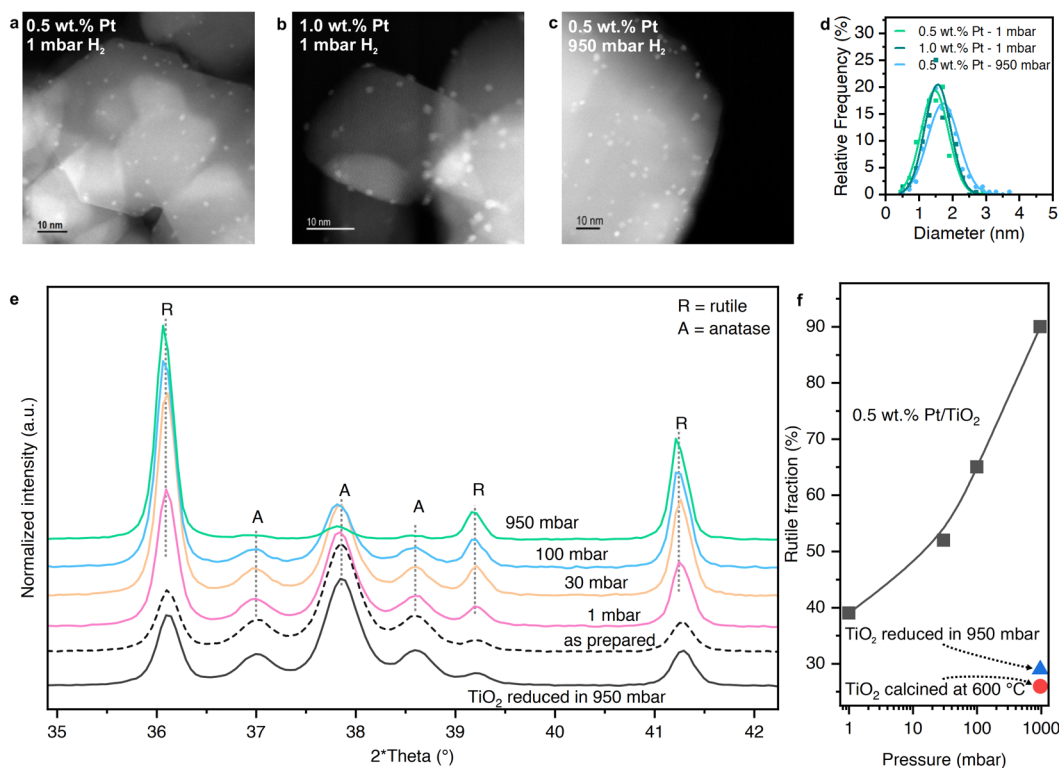


Figure 2. Catalyst structure. Representative TEM micrographs of the platinum–titania catalysts after the TPR experiment at the respective pressure: (a) 0.5 wt % Pt/TiO₂ after TPR to 700 °C at 1 mbar of hydrogen; (b) 1.0 wt % Pt/TiO₂ after TPR at 1 mbar of hydrogen; (c) 0.5 wt % Pt/TiO₂ after TPR at 700 mbar of hydrogen. (d) Platinum particle size distributions ($N = 200$) after the TPR. (e) Ex situ X-ray diffraction patterns of the 0.5 wt % Pt/TiO₂ catalyst after the H₂-TPR to 973 K. (f) Phase transformation of anatase to rutile titania can be observed, which is depicted as the fraction of rutile present in titania. As reference, bare titania is also displayed after calcination and after the H₂-TPR at 950 mbar and 973 K.

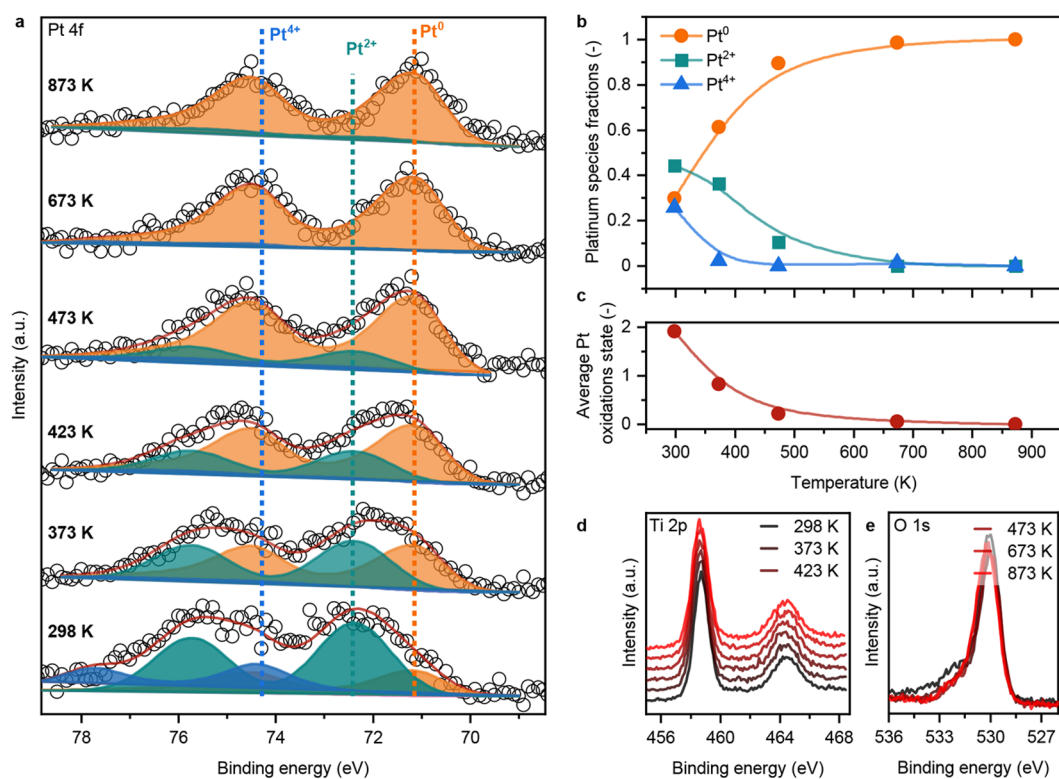


Figure 3. In situ X-ray photoemission spectroscopy of the 1.0 wt % Pt/TiO₂ catalyst: Pt 4f (a), Ti 2p (d), and O 1s (e) spectra acquired in 1 mbar of hydrogen while stepwise increasing the temperature. The spectra were collected at a photon energy of 1000 eV. (b) Fractions of Pt⁰, Pt²⁺, and Pt⁴⁺ determined by peak fitting of the Pt 4f spectra. (c) Average oxidation state of platinum during the temperature-programmed reduction.

studied temperature of 973 K. While the amount of hydrogen uptake below 373 K is almost linearly dependent on the platinum content, the high-temperature features show only a weak dependence of the platinum content.

At 1 mbar and temperatures below 473 K, the 1.0 wt % Pt catalyst shows a similar behavior compared to the higher pressures. However, the uptake is now characterized by three peaks instead of two. This shows that there are certain consecutive reduction processes which are better revealed or present at 1 mbar. At higher temperature, the uptake level is much lower compared to all other pressures and approaches zero as the measurement reaches 973 K. The 0.5 wt % Pt catalyst strongly deviates in its reduction behavior. There is only a very small hydrogen uptake peak at 373 K, and the first significant uptake is observed at the much higher temperature of 673 K. Beyond this feature, the uptake behavior follows the one of the 1.0 wt % Pt catalyst at 1 mbar.

To correlate these observations to structure, the catalyst was examined by means of scanning transmission electron microscopy (Figure 2a–d). Here, after the TPR experiments of most extreme cases (1 and 950 mbar), the catalysts were examined for their respective platinum nanoparticle sizes. The micrographs revealed in all cases a homogeneous distribution of small platinum nanoparticles. The particle size after reduction of the 1.0 wt % Pt catalyst at 950 mbar was 0.1–0.2 nm larger (1.7 ± 0.5 nm) compared to their 1 mbar counterpart (1.5 ± 0.4 nm for 0.5 wt % Pt and 1.6 ± 0.4 nm for 1 wt % Pt), hardly significant. This indicates that the hydrogen pressure only has a minor influence on the degree of sintering. To get a deeper understanding of the transformations which may occur within the titania structure, ex

situ X-ray powder diffraction (XRD) patterns of the catalysts after the TPR experiments were collected (Figure 2e).

The crystal structure of calcined titania P25 without platinum was also studied after the reduction at 950 mbar. After high-temperature reduction, the diffraction pattern of this bare titania shows the characteristic anatase to rutile ratio for P25 (Figure 2f). Among the samples with 0.5 and 1.0 wt % Pt no differences in the diffraction pattern were observed; for simplicity reasons only the 0.5 wt % Pt samples are shown. The diffraction patterns show a decrease of the anatase reflections between 37° and 39° and a rise of the reflections related to the rutile crystal structure at 36.2°, 39.5°, and 41.5°. The transformation of the anatase structure into rutile is thermodynamically favored,²⁶ and throughout the experiment an increasing fraction of rutile is observed with increased pressure (Figure 2f). Using 950 mbar of hydrogen, the transformation of anatase is almost completed. The titania structure consequently depends on the applied reductive conditions.

To identify the chemical state of the initial platinum particles and to capture potential surface reduction of the titania support, in situ XPS was performed on the 1.0 wt % catalyst at 1 mbar of hydrogen, close to the maximum pressure which can be routinely achieved at soft X-ray synchrotron beamlines. The respective Pt 4f, Ti 2p, and O 1s spectra acquired at 1000 eV photon energy and the evolution of the platinum speciation achieved by spectra fitting are depicted in Figure 3. The initial Pt 4f spectrum can be deconvoluted by three species, namely, Pt⁰ at 71.1 eV, Pt²⁺ at 72.4 eV, and Pt⁴⁺ at 74.4 eV. Already the initial spectrum shows a significant contribution of metallic platinum (30%), while contributions from Pt²⁺ (42%) and Pt⁴⁺ (28%) can be found. This results in an averaged oxidation state

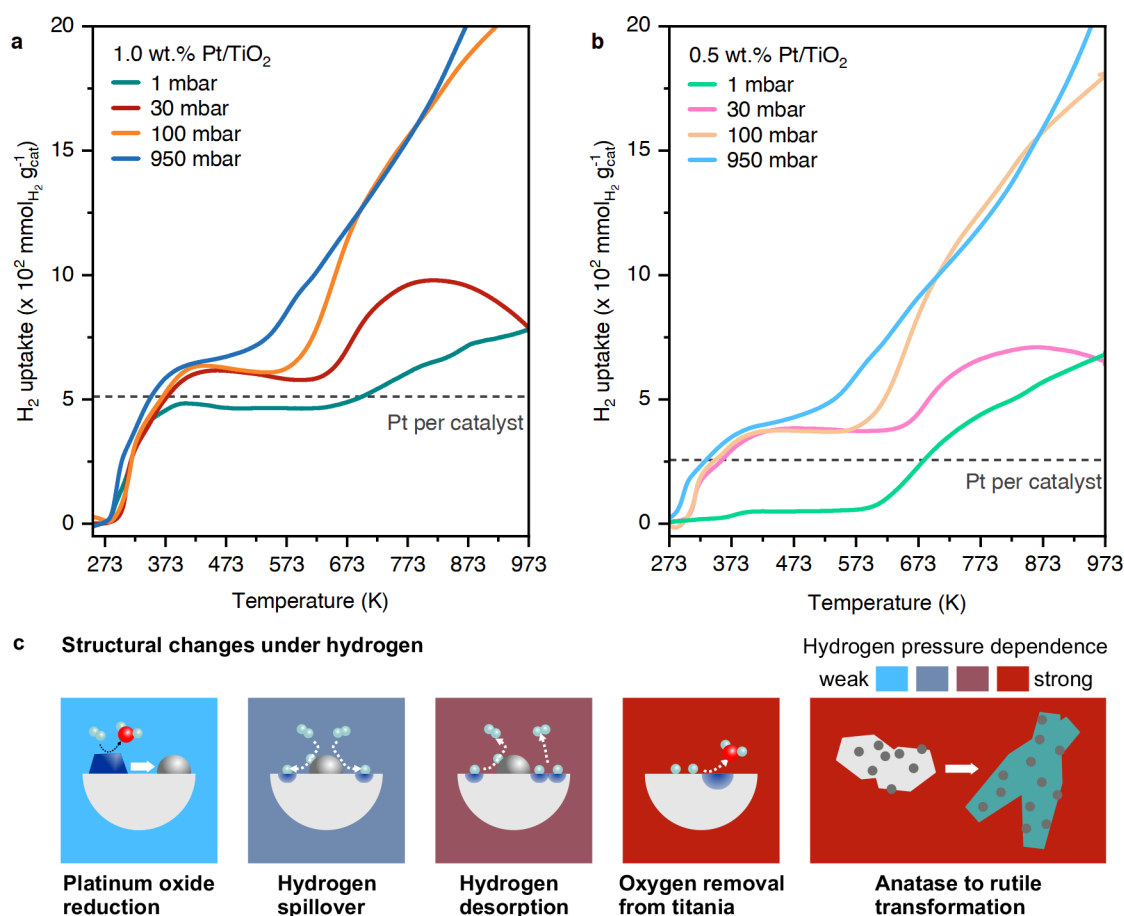


Figure 4. Hydrogen uptake. Total hydrogen uptake for the 1.0 wt % (a) and 0.5 wt % (b). The dashed line indicates the amount of platinum per mass of catalyst for the two different weight loadings. (c) Schematic of the hydrogen-induced structural transformations ranked by their dependence on the hydrogen pressure.

of 2 (Figure 3c). That is well in line with the estimated presence of PtO_{1.2} quantified by the TPR measurements. As the temperature is increased, the resonances of Pt⁴⁺ almost fully disappear when heated to 373 K, while those of Pt²⁺ undergo minor reduction. Further increase in temperature leads to their consumption, and above 473 K only contributions of metallic platinum are observed. This is in good agreement with the observations made by the TPR measurements. Consequently, hydrogen uptake beyond 473 K can be attributed to interaction with the titania substrate. However, the Ti 2p spectra do not show any sign of Ti³⁺ at any temperature up to 873 K (Figure 3d), which would represent a low-energy feature at around 457 eV.²⁷ Also, the O 1s spectra (Figure 3e), which is sensitive to the presence of hydroxyls, showed the initial presence of a small low-energy peak which can be associated with the formation of hydroxyls; however, at 373 K this peak decreased in intensity, and the spectra remained unchanged throughout all studied temperatures.

DISCUSSION

The comparison of titania P25 with Pt/TiO₂ (Figures 1 and 2e) shows that the platinum–titania interface has to be present to trigger pronounced titania reduction by hydrogen. The gained understanding on the structural transformations which occur during reduction within Pt/TiO₂ can be discussed in a quantitative manner. The integration of the TPR profiles yields

the cumulated hydrogen uptake of the various experiments (Figure 4). This allows direct comparison of the experiments performed at different pressures. As the average initial oxidation state was determined to be 2, the ratio of hydrogen to platinum necessary to fully reduce platinum is 1:1; consequently, the gray dashed line in Figure 4 shows this nominal ratio. As already seen, qualitatively in Figure 1, the initial reduction of platinum in between 273 and 423 K is virtually the same for all pressures. This can be explained by the high adsorption energy of hydrogen on platinum and platinum oxide, making the initial reduction process close to zero order in the studied pressure range. The two peaks contributing to the reduction may be related to the reduction of Pt⁴⁺ species and consequently the reduction of Pt²⁺ species as seen by XPS.

Beyond the platinum reduction, the hydrogen pressure has a strong influence on the further uptake of hydrogen. At 30 mbar and above, the hydrogen uptake slightly exceeds the amount necessary for platinum reduction. This uptake can be assigned to interfacial reduction and hydrogen spillover. As the temperature is increased, the samples treated at 30 and 100 mbar show desorption of hydrogen from the sample. This was previously observed in similar experiments.²³ With rising temperature, hydrogen adsorption is becoming less favorable due to the increase of entropy in the gas phase. Therefore, hydrogen can desorb in temperature-programmed experi-

Table 1. $\text{Ti}^{3+}/\text{Ti}^{4+}$ Based on the Hydrogen Uptake beyond 473 K

hydrogen partial pressure (mbar)	$\text{Ti}^{3+}/\text{Ti}^{4+}$ ratio at 773 K		$\text{Ti}^{3+}/\text{Ti}^{4+}$ ratio at 873 K		$\text{Ti}^{3+}/\text{Ti}^{4+}$ ratio at 973 K	
	0.5 wt %	1.0 wt %	0.5 wt %	1.0 wt %	0.5 wt %	1.0 wt %
1	1.0×10^{-3}	8.2×10^{-4}	2.3×10^{-3}	1.6×10^{-3}	2.4×10^{-3}	2.1×10^{-3}
30	2.4×10^{-3}	2.3×10^{-3}	2.7×10^{-3}	2.3×10^{-3}	2.4×10^{-3}	1.2×10^{-3}
100	5.9×10^{-3}	6.1×10^{-3}	7.7×10^{-3}	8.4×10^{-3}	9.4×10^{-3}	9.0×10^{-3}
950	5.9×10^{-3}	6.1×10^{-3}	8.4×10^{-3}	9.8×10^{-3}	1.2×10^{-2}	1.5×10^{-2}

ments. At 1 mbar, the 1.0 wt % Pt catalyst shows a similar hydrogen uptake; however, the total uptake of hydrogen does not exceed the nominal uptake necessary for platinum reduction. This is in line with the absence of any Ti^{3+} in the XPS signal.

As the temperature is further increased, the ion mobility in the titania increases. It was reported that there is a strong increase in ion mobility above 700 K.²⁸ In this regime reduced Ti^{3+} interstitials start to exchange with Ti^{4+} cations from the bulk.²⁸ In our experiments, we observe that the second strong uptake of hydrogen starts to occur at 673 K for pressures of 30 mbar and above. Given that this is the onset temperature of surface-bulk ion exchange, it seems that this mobility is required to induce a further reduction of the titania. Only at 950 mbar is greater reduction already observed at lower temperatures. For 30 mbar and at temperatures beyond 773 K, a release of hydrogen was observed. Because of this release, the total uptake in the 30 mbar case decreases, by 973 K, to the level of the 1 mbar TPR. As described earlier, thermodynamic stable hydrogen coverage is continuously decreasing when the temperature is raised; however, a certain fraction of hydroxyls remain stable up to the studied temperatures.²⁹ Higher hydrogen pressure stabilizes these hydroxyls, so at lower pressure some of the hydroxyls decompose and desorb in the form of hydrogen, while at higher pressures no desorption is distinguished.

Based on the hydrogen uptake beyond a hydrogen to platinum ratio of 1, the theoretical titania reduction can be calculated. The $\text{Ti}^{3+}/\text{Ti}^{4+}$ ratio (Table 1) beyond 773 K shows very similar values for both catalysts at each respective pressure. This shows that the degree of reduction is independent of the surface platinum concentration. However, a platinum–titania interface is required since no comparable reduction was observed in the absence of platinum. The $\text{Ti}^{3+}/\text{Ti}^{4+}$ ratio is increasing with the pressure; this increase in reduction is correlated to the observed anatase-to-rutile transition, which also increases with hydrogen pressure. However, the $\text{Ti}^{3+}/\text{Ti}^{4+}$ ratio does not exceed 1% (950 mbar, 973 K). Consequently, the detection of titania reduction in powder catalysts is extremely challenging. In close agreement with our data, electron paramagnetic resonance measurements, which are sensitive to such low concentrations, quantified the $\text{Ti}^{3+}/\text{Ti}^{4+}$ ratio to be 3.5×10^{-3} for similar catalyst and reduction conditions.^{30,31} Surface-sensitive techniques like XPS, however, currently suffer from the pressure limitations to follow this process in situ as it becomes apparent when comparing the present XPS data and the TPR data. Below 773 K negligible titania reduction occurs. Titania reduction at 1 mbar is observed beyond 773 K, a temperature where fast surface-bulk exchange occurs and the majority of Ti^{3+} cations will reside in the bulk, thus invisible for XPS.

Applying different pressures will lead to different structures, and the pressure gap results in a materials gap. Yet, titania is one of the classical systems studied by XPS in the past, and

numerous reports exist that report titania reduction seen by XPS.^{32,33} However, in these studies, the reduction of titania is usually not induced by molecular hydrogen but either by ion bombardment or high-temperature annealing under ultrahigh-vacuum conditions. Both procedures may have a much stronger reductive influence on titania. In addition, very often single crystals of titania surfaces were studied which potentially results in a different interaction with hydrogen compared to the complex structure of powder titania.

At 1 mbar, the behaviors of the two catalysts are fundamentally different. At this pressure, distinctive differences between the two weight loadings appear. At lower weight loadings, platinum atoms occupy stronger adsorption sites.^{34,35}

At 1 mbar, their difference in reducibility results in substantially higher temperatures ($\Delta T = 300$ K) for the 0.5 wt % catalyst compared to the 1.0 wt % catalyst. In opposition, at hydrogen pressures 1 order of magnitude higher, those differences vanish.

It has to be noted that the formation of an SMSI overlayer around the platinum nanoparticles due to high-temperature reduction is very likely to occur.^{19,20,36} Such an overlayer will influence the behavior of hydrogen adsorption and spillover. The degree of overlayer formation and its structure are a complex function of temperature and hydrogen pressure. A detailed investigation of this phenomenon exceeds the frame of this work and has to be addressed in the future to unify specific findings in the field of overlayer formation.

CONCLUSION

In summary, there is an omnipresent effect of hydrogen pressure on the hydrogen uptake kinetics and the consecutive structural transformations of platinum–titania catalysts (Figure 4c). The reduction of the platinum oxide phase becomes pressure-independent at pressures above 30 mbar. Yet, the related spillover of hydrogen and its stability on the titania are a function of pressure. Higher pressures promote higher hydrogen uptake and prevent desorption of hydrogen from the catalyst. At around 673 K, the major hydrogen uptake due to titania reduction occurs at all pressures; this temperature correlates to the onset of high ion mobility in titania. The degree to which this proceeds is dependent on the pressure. Finally, the transformation of the anatase phase into the rutile phase of the titania support strongly depends on pressure; the higher the hydrogen pressure, the larger the extent of transformation. Comparing the same material studied at two different pressures will lead to different structures and consequently may produce seemingly contradicting results. As shown here, methods that can bridge such pressures help to align and harmonize such findings. In addition, such findings allow the adjustment of treatment and/or reaction conditions to a desired material state.

AUTHOR INFORMATION

Corresponding Author

Jeroen A. van Bokhoven – Institute for Chemical and Bioengineering (ICB), ETH Zurich, 8093 Zurich, Switzerland; Laboratory for Catalysis and Sustainable Chemistry (LSK), Paul Scherrer Institute, 5232 Villigen, Switzerland; orcid.org/0000-0002-4166-2284; Phone: +41 44 632 55 42; Email: jeroen.vanbokhoven@chem.ethz.ch

Authors

Arik Beck – Institute for Chemical and Bioengineering (ICB), ETH Zurich, 8093 Zurich, Switzerland; orcid.org/0000-0001-5267-3141

Hannes Frey – Scientific Center for Optical and Electron Microscopy (ScopeM), ETH Zurich, 8093 Zurich, Switzerland

Matthias Becker – Institute for Chemical and Bioengineering (ICB), ETH Zurich, 8093 Zurich, Switzerland

Luca Artiglia – Laboratory for Catalysis and Sustainable Chemistry (LSK), Paul Scherrer Institute, 5232 Villigen, Switzerland; orcid.org/0000-0003-4683-6447

Marc G. Willinger – Scientific Center for Optical and Electron Microscopy (ScopeM), ETH Zurich, 8093 Zurich, Switzerland; orcid.org/0000-0002-9996-7953

Complete contact information is available at:
<https://pubs.acs.org/10.1021/acs.jpcc.1c05939>

Notes

The authors declare no competing financial interest.

ACKNOWLEDGMENTS

A.B. and J.A.v.B. acknowledge the SNSF project 200021_178943 for funding. The Swiss Light Source is acknowledged for beam time at the in situ spectroscopy beamline (proposal 20190861).

REFERENCES

- (1) Cargnello, M.; Fornasiero, P.; Gorte, R. J. Playing with Structures at the Nanoscale: Designing Catalysts by Manipulation of Clusters and Nanocrystals as Building Blocks. *ChemPhysChem* **2013**, *14* (17), 3869–3877.
- (2) Nagai, Y.; Dohmae, K.; Ikeda, Y.; Takagi, N.; Tanabe, T.; Hara, N.; Guiler, G.; Pascarelli, S.; Newton, M. A.; Kuno, O.; et al. In Situ Redispersion of Platinum Autoexhaust Catalysts: An On-Line Approach to Increasing Catalyst Lifetimes? *Angew. Chem., Int. Ed.* **2008**, *47* (48), 9303–9306.
- (3) Nagai, Y.; Dohmae, K.; Ikeda, Y.; Takagi, N.; Hara, N.; Tanabe, T.; Guiler, G.; Pascarelli, S.; Newton, M. A.; Takahashi, N.; et al. In Situ Observation of Platinum Sintering on Ceria-Based Oxide for Autoexhaust Catalysts Using Turbo-XAS. *Catal. Today* **2011**, *175* (1), 133–140.
- (4) Bañares, M. A. Operando Spectroscopy: The Knowledge Bridge to Assessing Structure-Performance Relationships in Catalyst Nanoparticles. *Adv. Mater.* **2011**, *23* (44), 5293–5301.
- (5) Roy, K.; Artiglia, L.; van Bokhoven, J. A. Ambient Pressure Photoelectron Spectroscopy: Opportunities in Catalysis from Solids to Liquids and Introducing Time Resolution. *ChemCatChem* **2018**, *10* (4), 666–682.
- (6) Tang, M.; Yuan, W.; Ou, Y.; Li, G.; You, R.; Li, S.; Yang, H.; Zhang, Z.; Wang, Y. Recent Progresses on Structural Reconstruction of Nanosized Metal Catalysts via Controlled-Atmosphere Transmission Electron Microscopy: A Review. *ACS Catal.* **2020**, *10*, 14419–14450.
- (7) Wagner, J. B.; Hansen, P. L.; Molenbroek, A. M.; Topsøe, H.; Clausen, B. S.; Helveg, S. In Situ Electron Energy Loss Spectroscopy Studies of Gas-Dependent Metal-Support Interactions in Cu/ZnO Catalysts. *J. Phys. Chem. B* **2003**, *107* (31), 7753–7758.
- (8) Liu, X.; Zhang, C.; Li, Y.; Niemantsverdriet, J. W.; Wagner, J. B.; Hansen, T. W. Environmental Transmission Electron Microscopy (ETEM) Studies of Single Iron Nanoparticle Carburization in Synthesis Gas. *ACS Catal.* **2017**, *7* (7), 4867–4875.
- (9) Hansen, J. B.; Højlund Nielsen, P. E. Methanol Synthesis. In *Handbook of Heterogeneous Catalysis*; Wiley-VCH Verlag GmbH & Co. KGaA: Weinheim, Germany, 2008; Vol. 2, pp 2920–2949.
- (10) Schlögl, R. Ammonia Synthesis. In *Handbook of Heterogeneous Catalysis*; Wiley-VCH Verlag GmbH & Co. KGaA: Weinheim, Germany, 2008; pp 2501–2575.
- (11) Hinrichsen, K.-O.; Kochloeff, K.; Muhler, M. Water Gas Shift and COS Removal. In *Handbook of Heterogeneous Catalysis*; Wiley-VCH Verlag GmbH & Co. KGaA: Weinheim, Germany, 2008; pp 2905–2920.
- (12) Urakawa, A. Mind the Gaps in CO₂-to-Methanol. *Nat. Catal.* **2021**, *4* (6), 447–448.
- (13) Imbihl, R.; Behm, R. J.; Schlögl, R. Bridging the Pressure and Material Gap in Heterogeneous Catalysis. *Phys. Chem. Chem. Phys.* **2007**, *9* (27), 3459.
- (14) Reece, C.; Redekop, E. A.; Karakalos, S.; Friend, C. M.; Madix, R. J. Crossing the Great Divide between Single-Crystal Reactivity and Actual Catalyst Selectivity with Pressure Transients. *Nat. Catal.* **2018**, *1* (11), 852–859.
- (15) Beck, A.; Zabilskiy, M.; Newton, M. A.; Safonova, O.; Willinger, M. G.; van Bokhoven, J. A. Following the Structure of Copper-Zinc-Alumina across the Pressure Gap in Carbon Dioxide Hydrogenation. *Nat. Catal.* **2021**, *4* (6), 488–497.
- (16) Lox, E. S. J. Automotive Exhaust Treatment. In *Handbook of Heterogeneous Catalysis*; Wiley-VCH Verlag GmbH & Co. KGaA: Weinheim, Germany, 2008; pp 2274–2345.
- (17) Liu, L.; Corma, A. Metal Catalysts for Heterogeneous Catalysis: From Single Atoms to Nanoclusters and Nanoparticles. *Chem. Rev.* **2018**, *118* (10), 4981–5079.
- (18) Tauster, S. J.; Fung, S. C.; Garten, R. L. Strong Metal-Support Interactions. Group 8 Noble Metals Supported on TiO₂. *J. Am. Chem. Soc.* **1978**, *100* (1), 170–175.
- (19) Beck, A.; Huang, X.; Artiglia, L.; Zabilskiy, M.; Wang, X.; Rzepka, P.; Palagin, D.; Willinger, M.-G.; van Bokhoven, J. A. The Dynamics of Overlayer Formation on Catalyst Nanoparticles and Strong Metal-Support Interaction. *Nat. Commun.* **2020**, *11* (1), 3220.
- (20) Zhang, Y.; Yang, X.; Yang, X.; Duan, H.; Qi, H.; Su, Y.; Liang, B.; Tao, H.; Liu, B.; Chen, D.; Su, X.; Huang, Y.; Zhang, T. Tuning Reactivity of Fischer-Tropsch Synthesis by Regulating TiOx Overlayer over Ru/TiO₂ Nanocatalysts. *Nat. Commun.* **2020**, *11* (1), 3185.
- (21) Corma, A.; Serna, P.; Concepción, P.; Calvino, J. J. Transforming Nonselective into Chemoselective Metal Catalysts for the Hydrogenation of Substituted Nitroaromatics. *J. Am. Chem. Soc.* **2008**, *130* (27), 8748–8753.
- (22) Artiglia, L.; Orlando, F.; Roy, K.; Kopelent, R.; Safonova, O.; Nachtegaal, M.; Huthwelker, T.; van Bokhoven, J. A. Introducing Time Resolution to Detect Ce³⁺ Catalytically Active Sites at the Pt/CeO₂ Interface through Ambient Pressure X-Ray Photoelectron Spectroscopy. *J. Phys. Chem. Lett.* **2017**, *8* (1), 102–108.
- (23) Huizinga, T.; Van Grondelle, J.; Prins, R. A Temperature Programmed Reduction Study of Pt on Al₂O₃ and TiO₂. *Appl. Catal.* **1984**, *10* (2), 199–213.
- (24) Levy, R.; Boudart, M. The Kinetics and Mechanism of Spillover. *J. Catal.* **1974**, *32* (2), 304–314.
- (25) Karim, W.; Spreafico, C.; Kleibert, A.; Gobrecht, J.; Vandevonede, J.; Ekinci, Y.; Van Bokhoven, J. A. Catalyst Support Effects on Hydrogen Spillover. *Nature* **2017**, *541* (7635), 68–71.
- (26) Shannon, R. D.; Pask, J. A. Kinetics of the Anatase-Rutile Transformation. *J. Am. Ceram. Soc.* **1965**, *48* (8), 391–398.

- (27) Lazarus, M. S.; Sham, T. K. X-Ray Photoelectron Spectroscopy (XPS) Studies of Hydrogen Reduced Rutile (TiO_{2-x}) Surfaces. *Chem. Phys. Lett.* **1982**, *92* (6), 670–674.
- (28) Henderson, M. A. A Surface Perspective on Self-Diffusion in Rutile TiO_2 . *Surf. Sci.* **1999**, *419*, 174–187.
- (29) Spreafico, C.; Karim, W.; Ekinci, Y.; van Bokhoven, J. A.; VandeVondele, J. Hydrogen Adsorption on Nanosized Platinum and Dynamics of Spillover onto Alumina and Titania. *J. Phys. Chem. C* **2017**, *121* (33), 17862–17872.
- (30) Chen, B. H.; White, J. M. Properties of Platinum Supported on Oxides of Titanium. *J. Phys. Chem.* **1982**, *86* (18), 3534–3541.
- (31) Chen, B. H.; White, J. M. Behavior of Ti^{3+} Centers in the Low-Temperature Reduction of Pt/ TiO_2 /K Systems. *J. Phys. Chem.* **1983**, *87* (8), 1327–1329.
- (32) Pan, J.-M.; Maschhoff, B. L.; Diebold, U.; Madey, T. E. Interaction of Water, Oxygen, and Hydrogen with TiO_2 (110) Surfaces Having Different Defect Densities. *J. Vac. Sci. Technol., A* **1992**, *10* (4), 2470–2476.
- (33) Sanjinés, R.; Tang, H.; Berger, H.; Gozzo, F.; Margaritondo, G.; Lévy, F. Electronic Structure of Anatase TiO_2 Oxide. *J. Appl. Phys.* **1994**, *75* (6), 2945–2951.
- (34) Thang, H. V.; Pacchioni, G.; DeRita, L.; Christopher, P. Nature of Stable Single Atom Pt Catalysts Dispersed on Anatase TiO_2 . *J. Catal.* **2018**, *367*, 104–114.
- (35) Resasco, J.; Derita, L.; Dai, S.; Chada, J. P.; Xu, M.; Yan, X.; Finzel, J.; Hanukovich, S.; Hoffman, A. S.; Graham, G. W.; et al. Uniformity Is Key in Defining Structure-Function Relationships for Atomically Dispersed Metal Catalysts: The Case of Pt/ CeO_2 . *J. Am. Chem. Soc.* **2020**, *142* (1), 169–184.
- (36) Wang, X.; Beck, A.; van Bokhoven, J. A.; Palagin, D. Thermodynamic Insights into Strong Metal-Support Interaction of Transition Metal Nanoparticles on Titania: Simple Descriptors for Complex Chemistry. *J. Mater. Chem. A* **2021**, *9* (7), 4044–4054.